Vibronically Induced Active Center in Photocatalyst: Jahn-Teller Effect in Vanadium Oxide Supported on Silica

Tohru Sato,[1,2,*] Naoya Iwahara,[3] Ken Tokunaga[†],[2]

Kazuyoshi Tanaka,[2,4] and Tsunehiro Tanaka[2]

[1]*Fukui Institute for Fundamental Chemistry, Kyoto University, Takano-Nishihiraki-cho 34-4, Sakyo-ku, Kyoto 606-8103, Japan*

[2]*Department of Molecular Engineering, Graduate School of Engineering, Kyoto University, Kyoto 615-8510, Japan*

[3]*Department of Engineering Chemistry, Faculty of Engineering, Kyoto University, Kyoto 615-8510, Japan*

[4]*Core Research for Evolutional Science and Technology, Japan Science and Technology Agency (JST-CREST)*

(Dated: Submitted on 26 February, 2008)

[†] Present address: Research and Development Center for Higher Education, Kyushu University, Fukuoka 810-8560, Japan

Abstract

The vibronic interactions in a photocatalyst, isolated vanadium oxide on silica (VO_4/SiO_2), is investigated. The coupling between the vibrational e mode and the electronic T_1 state induces a charge transfer from the basal oxygens to the terminal oxygen. The T_1 state gives rise to a Jahn-Teller (JT) distortion after the excitation. The HOMO of the JT distorted molecule, which is localized on the active center, the terminal oxygen, is destabilized against the JT distortion, while the system is stabilized because of the JT effect. The destabilization and localization of the HOMO may cause enhancement of the reactivity for the oxidation.

I. INTRODUCTION

Highly dispersed vanadium oxide on silica, VO_4/SiO_2, is a photocatalyst which promotes the oxidation of light alkenes.[1–4] The active species is the isolated VO_4, which has a C_{3v} structure (see FIG. 1(a)).[5] The vanadium oxide has two kinds of oxygen, basal oxygen (O_b) and terminal oxygen (O_t). The terminal oxygen reacts with a substrate in the photo-excited T_1 state.[2,3,6] Spectroscopy and molecular orbital calculation have revealed that the HOMO of the ground state consists of p orbitals of the basal oxygens, and LUMO's are doubly degenerate orbitals which originated from d orbitals of vanadium.[7,8] The first triplet state is assigned to the excitation from the HOMO to the LUMO.[8]

In the T_1 state, the frontier orbitals have no orbital coefficient on the terminal oxygen, although a substrate reacts with the terminal oxygen. In addition, a driving force of the ligand-to-metal charge transfer (LMCT) from the terminal oxygen to the vanadium is still open.[7]

In this Letter, we will address these problems in terms of the vibronic coupling theory[9–11] using the density functional calculation and the model calculation.

II. STRUCTURES

We employed H_3VO_4 as a model of the isolated VO_4 on silica (VO_4/SiO_2), where three Si atoms bonded with the O_b are replaced by hydrogen atoms (FIG. 1(b)). We optimized the singlet ground state and the triplet state of H_3VO_4 using the density functional method. We employed the B3LYP functional with a basis set, LANL2DZ for V, 6-31G(d) for O, and 6-31G for H. To obtain vibrational modes and frequencies, vibrational analyses were performed. For simplicity, we adopted the result of the ground state as vibrational modes

of the present system. Molecular orbitals were obtained employing the extended Hückel method. All the density functional calculations and the extended Hückel calculations were performed using the Gaussian03 package.[12]

For the ground state, we optimized the structure within the C_{3v} symmetry. The vibrational frequencies are tabulated in Table I, and the vibrational a_1 and e modes are depicted in FIG. 2. One imaginary mode $a_2(1)$ remains in the C_{3v}-optimized structure, which will give rise to a distortion from C_{3v} to C_3 or lower symmetry. It is ascribed to the pseudo Jahn–Teller effect in the ground state. Since this effect is not important in the present discussion, we simply refer the optimized structure within the C_{3v} symmetry as the optimized structure.

On the other hand, for the triplet state, we obtained two C_s structures, one is a local minimum, and the other a saddle point with one imaginary frequency. Figure 3 shows a schematic representation of the potential surface of the triplet state. At the middle, the potential surfaces conically intersect, and the minima are located along the trough which corresponds to the deformed structures. The minima are separated by the saddle points. This suggests that the Jahn–Teller effect occurs in the triplet state, and the vibronic coupling may play an important role in the mechanism of the photocatalytic reaction. In fact, in the C_s structure, the frontier orbitals have finite coefficients on the terminal oxygen, while, in the C_{3v} structure, the HOMO has no coefficient on the terminal oxygen at all. Therefore, the reaction center appears, and the LMCT occurs associated with the Jahn-Teller distortion. In other words, the vibronic coupling induces the active center of the photocatalyst. The effects on the frontier orbitals are discussed in detail in Sec. III.

Since the electronic term of the photo-excited state is ^3E, the Jahn–Teller active vibra-

tional modes are deduced from the symmetric product representation:

$$\left[E^2\right] = a_1 \oplus e.$$

Thus, the Jahn–Teller active mode is an e mode. In the model molecule, H_3VO_4, there are five a_1 and six e modes. Among them, some vibrational modes significantly couple to the electronic state. To find such modes, the distortion from the ground state structure with the C_{3v} symmetry to the triplet state with the C_s symmetry was projected onto these vibrational modes. The result is summarized in Table II. It is found that the $e(3)$ mode has the largest contribution to the Jahn–Teller distortion. Thus, we concentrate ourselves on the $e(3)$ mode, for simplicity.

The a_1 modes also couple to the electronic state, though they cannot lower the molecular symmetry, and they shift the orbital levels. Therefore, they can contribute to the deformation associated with the transition from the singlet ground state to the triplet state. Among them, the $a_1(4)$ mode is particularly important since it corresponds to a stretching mode of the V=O_t bonds which has been attributed to the progression in the emission spectra.[6,13,14]

III. VIBRONIC MODEL

Figure 4 shows the change of the HOMO and NHOMO along the $e(3)$ mode which has the largest contribution in the JT deformation. Note that we denote HOMO, next HOMO (NHOMO), and LUMO as those of the singlet ground state, not the triplet state, throughout this Letter. The orbital patterns and levels were calculated using the extended Hückel method in the DFT optimized structures.[12] The LUMO's originate from the d orbitals of the vanadium, and they are doubly degenerate, which results in the Jahn-Teller effect after the electronic excitation $E \leftarrow A_1$. In the NHOMO, the molecular orbital is localized on

the terminal oxygen as well as the basal oxygens. The HOMO consists of the p orbitals of the basal oxygens and has no coefficients on the terminal oxygen as long as the molecular symmetry is C_{3v}. From Figure 4, it is clear that the finite coefficient on the terminal oxygen appears in the HOMO with the $e(3)$ deformation. Since the deformation and the level shifting depend on the vibronic coupling, we will estimate the orbital vibronic couplings between these orbitals and the $e(3)$ vibrational mode.

Since the LUMO level is doubly degenerate, denoted by e^*, the Jahn-Teller coupling exists between the LUMO's, denoted by $|\theta^*\rangle$ and $|\epsilon^*\rangle$. In addition, the NHOMO's are also e, and they are denoted by $|\theta\rangle$ and $|\epsilon\rangle$. The NHOMO's also couple to the e mode.

The Jahn–Teller active e mode can couple the e orbitals with a_2 and a_1 orbitals:

$$a_1 \otimes e = e, \quad a_2 \otimes e = e. \tag{1}$$

Therefore, such off-diagonal couplings should be taken into account in the present model. Since an off-diagonal coupling is important as long as two levels are close, we consider the off-diagonal couplings between the HOMO (a_2) and NHOMO (e), and that between the NHOMO and HOMO-2 (a_1).

Accordingly, we set up the following vibronic Hamiltonian:

$$\hat{H} = \hat{H}_0 + \hat{H}_{\rm LJT} + \hat{H}_{\rm off-diag} \tag{2}$$

$$\hat{H}_0 = \sum_i \epsilon_i |i\rangle\langle i|, \tag{3}$$

$$\begin{aligned} \hat{H}_{\rm LJT} \;=\; & V_1 \left[\left(-|\theta^*\rangle\langle\theta^*| + |\epsilon^*\rangle\langle\epsilon^*| \right) Q_\theta + \left(|\theta^*\rangle\langle\epsilon^*| + |\epsilon^*\rangle\langle\theta^*| \right) Q_\epsilon \right] \\ & + V_3 \left[\left(-|\theta\rangle\langle\theta| + |\epsilon\rangle\langle\epsilon| \right) Q_\theta + \left(|\theta\rangle\langle\epsilon| + |\epsilon\rangle\langle\theta| \right) Q_\epsilon \right], \end{aligned} \tag{4}$$

$$\begin{aligned} \hat{H}_{\rm off-diag} \;=\; & V_2 \left[\left(|a_2\rangle\langle\epsilon| + |\epsilon\rangle\langle a_2| \right) Q_\theta + \left(-|a_2\rangle\langle\theta| - |\theta\rangle\langle a_2| \right) Q_\epsilon \right] \\ & + V_4 \left[\left(|a_1\rangle\langle\theta| + |\theta\rangle\langle a_1| \right) Q_\theta + \left(|a_1\rangle\langle\epsilon| + |\epsilon\rangle\langle a_1| \right) Q_\epsilon \right], \end{aligned} \tag{5}$$

where $i = a_1, \theta, \epsilon, a_2, \theta^*, \epsilon^*$, and ϵ_i denotes the orbital level of the molecular orbital i. $\hat{H}_0$ is the Hamiltonian without a distortion. $\hat{H}_{\mathrm{LJT}}$ describes the linear Jahn–Teller couplings of the e^* and e orbitals, respectively. $\hat{H}_{\mathrm{off-diag}}$ describes the off-diagonal coupling between the e and a_2 orbitals and that between the e and a_1 orbitals. V_1, V_2, V_3, and V_4 denote the corresponding orbital vibronic coupling constants.

We obtained the orbital vibronic coupling constants for the $e(3)$ mode by fitting the eigenvalues of the above Hamiltonian (2) to the orbital energy levels calculated using the extended Hückel method. The calculated constants are $V_1 = 1.5 \times 10^{-1}$ eV/(amu$^{1/2}$·Å), $V_2 = 6.5 \times 10^{-2}$ eV/(amu$^{1/2}$·Å), $V_3 = 1.2 \times 10^{-2}$ eV/(amu$^{1/2}$·Å), $V_4 = 2.1 \times 10^{-2}$ eV/(amu$^{1/2}$·Å).

Figure 5 shows the eigenvalues of the vibronic Hamiltonian (2) with the parameters calculated above (solid lines) and the orbital level from the extended Hückel calculation (dotted lines). It is found that the Jahn-Teller stabilization mainly comes from the Jahn-Teller coupling V_1 of the LUMO e^*. Furthermore, the HOMO a_2 is slightly destabilized against the Jahn-Teller distortion with the off-diagonal coupling V_2. The HOMO which has no coefficient on the O_t interacts with the NHOMO e via the Jahn–Teller-active mode e. Figure 4 shows the orbital mixing of the HOMO and NHOMO. In other words, the whole system is stabilized by the Jahn-Teller coupling V_1, and, in the same time, the active center is induced by the off-diagonal vibronic coupling V_2 between the HOMO and NHOMO.

IV. CONCLUSION

We calculated the optimized structure in the singlet ground and triplet excited states of the model molecule of vanadium oxide on silica, and the energy spectrum of the vibronic Hamiltonian. Major findings are as follows:

1. The optimized structures of the triplet state have C_s symmetry, which is ascribed to the Jahn-Teller effect.

2. The Jahn-Teller stabilization mainly comes from the orbital vibronic coupling of the LUMO e^* originated from the d orbitals of the vanadium with the e vibrational mode.

3. The off-diagonal vibronic coupling V_2 induces the active center in the photocatalytic reaction, while the whole system is stabilized with the Jahn-Teller coupling V_1.

Since the a_1 and e modes couple to the phosphorescent state, the emission spectrum should shed light on the vibronic structure in the present system. In the assignments published so far, explaining the various separations of the vibrational fine structure have failed since they have considered only the stretching of V=O_t bond ($a_1(4)$ mode)[6,13,14] or attributed the progression to a stretching of the V-O-Si ligands.[8]

Our study reveals the crucial role of the e modes as well as the a_1 modes in the phosphorescent state. Further study on the complete assignment of the phosphorescence spectra is now in progress. The result will be published in the future.

Acknowledgments

Numerical calculation was partly performed in the Supercomputer Laboratory of Kyoto University and Research Center for Computational Science, Okazaki, Japan.

---

* tsato@scl.kyoto-u.ac.jp

[1] S. Yoshida, Y. Magatani, S. Noda, and T. Funabiki, Chem. Commun., 601 (1981).

[2] S. Yoshida, T. Tanaka, M. Okada, and T. Funabiki, J. Chem. Soc. Faraday Trans. **80**, 119 (1984).

[3] T. Tanaka, M. Ooe, T. Funabiki, and S. Yoshida, J. Chem. Soc. Faraday Trans. **82**, 35 (1986).

[4] F. Amano, T. Tanaka, and T. Funabiki, Langmuir **20**, 4236 (2004).

[5] S. Yoshida, T. Tanaka, T. Hanada, T. Hiraiwa, H. Kanai, and T. Funabiki, Catal. Lett. **12**, 277 (1992).

[6] A. M. Gritscov, V. A. Shvets, and V. B. Kazansky, Chem. Phys. Lett. **35**, 511 (1975).

[7] H. Kobayashi, M. Yamaguchi, T. Tanaka, and S. Yoshida, J. Chem. Soc., Faraday Trans. **81**, 1513 (1985).

[8] K. Tran, M. A. Hanning-Lee, A. Biswas, A. E. Stiegman, and G. W. Scott, J. Am. Chem. Soc. **117**, 2618 (1995).

[9] I. B. Bersuker, *The Jahn-Teller Effect and Vibronic Interactions in Modern Chemistry* (Plenum, NewYork, 1984).

[10] I. B. Bersuker and V. Z. Polinger, *Vibronic Interaction in Molecules and Crystals* (Springer, Berlin, 1989).

[11] I. B. Bersuker, *The Jahn-Teller Effect* (Cambridge University Press, Cambridge, 2006).

[12] M. J. Frisch, G. W. Trucks, H. B. Schlegel, G. E. Scuseria, M. A. Robb, J. R. Cheeseman, J. A. Montgomery, Jr., T. Vreven, K. N. Kudin, J. C. Burant, et al., *Gaussian 03, Revision C.02*, Wallingford CT (2004).

[13] M. Anpo, I. Tanahashi, and Y. Kubokawa, J. Phys. Chem. **84**, 3440 (1980).

[14] M. Iwamoto, H. Furukawa, K. Matsukami, T. Takenaka, and T. Kagawa, J. Am. Chem. Soc. **105**, 3719 (1983).

TABLE I: Vibrational frequency (cm^{-1}) of X^1A_1 sate of H_3VO_4. The asymmetric $a_2(1)$ mode with an imaginary frequency suggests that the pseudo Jahn-Teller effect occurs in the singlet ground state.

$a_1(1)$	255.4	$a_2(1)$	$124.0i$	$e(1)$	216.6
$a_1(2)$	698.2			$e(2)$	294.4
$a_1(3)$	758.7			$e(3)$	407.1
$a_1(4)$	1151.7			$e(4)$	637.7
$a_1(5)$	3763.6			$e(5)$	799.9
				$e(6)$	3756.4

TABLE II: Distortion of H_3VO_4 in the T_1 state from C_{3v} to C_s projected on the normal coordinates ($\sqrt{\text{amu}}$Å).

$a_1(1)$	0.330	$e(1)$	-0.039
$a_1(2)$	0.390	$e(2)$	-0.567
$a_1(3)$	0.438	$e(3)$	1.397
$a_1(4)$	0.607	$e(4)$	0.149
$a_1(5)$	-0.616	$e(5)$	0.132
		$e(6)$	0.436

(a) (b)

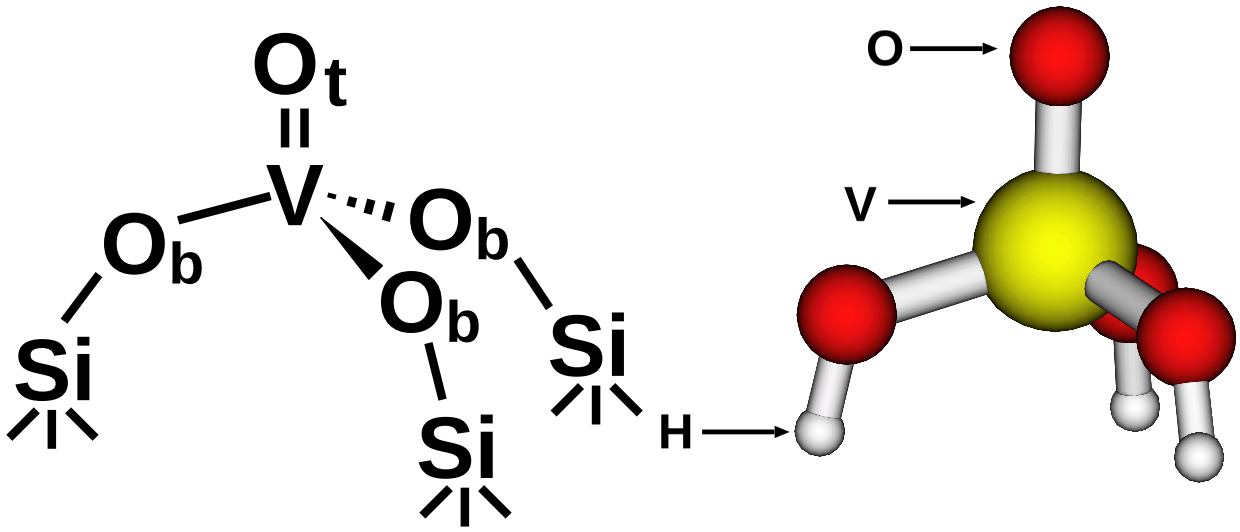

FIG. 1: Sato et. al

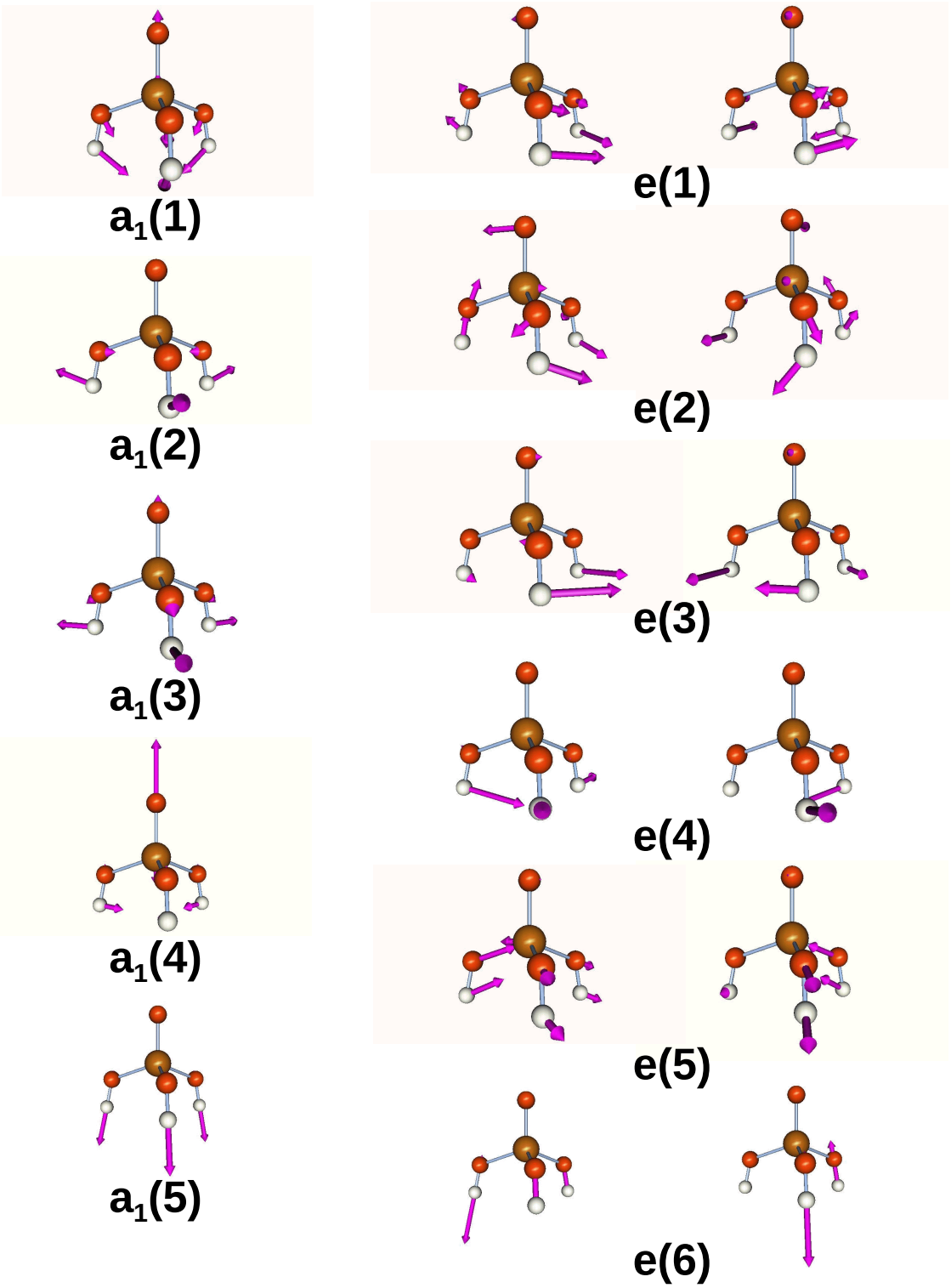

FIG. 2: Sato et. al

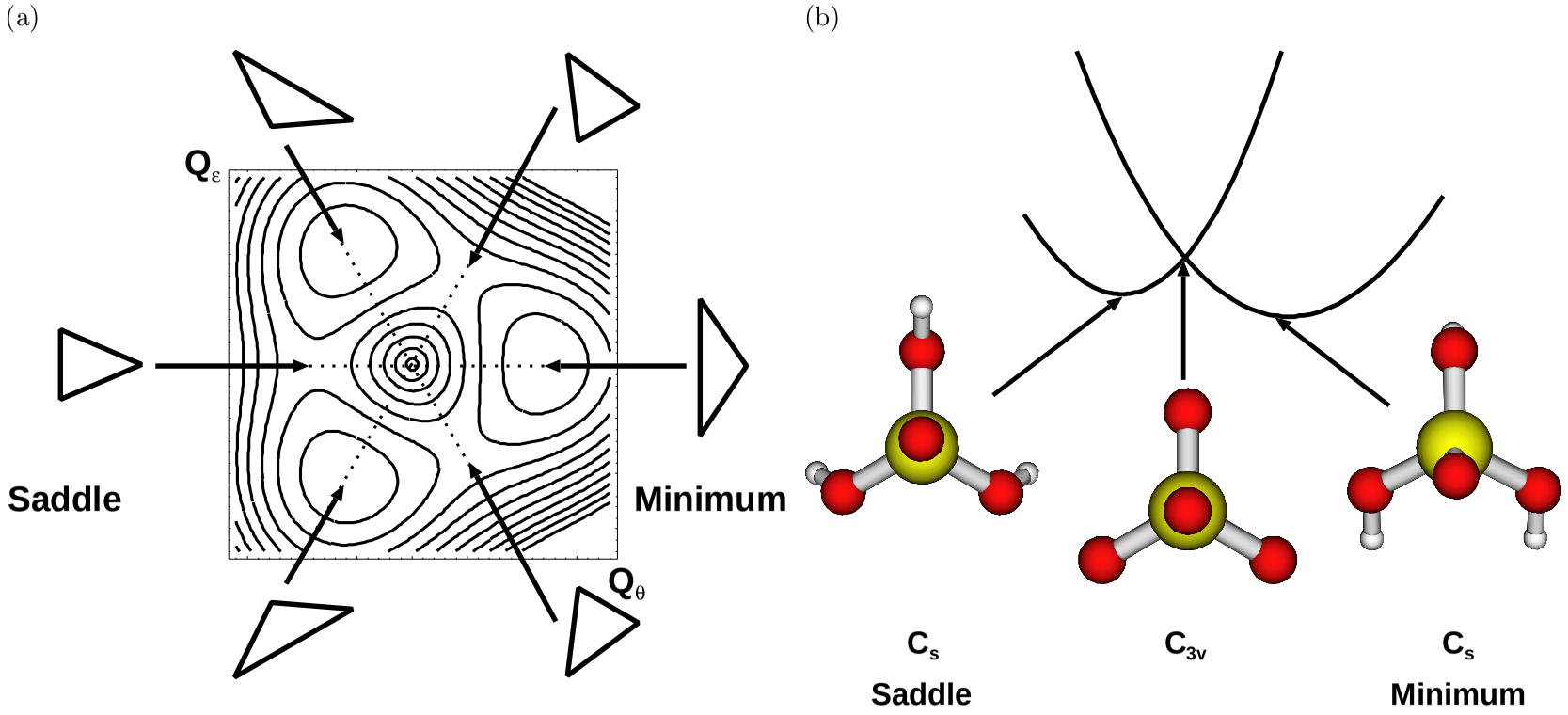

FIG. 3: Sato et. al

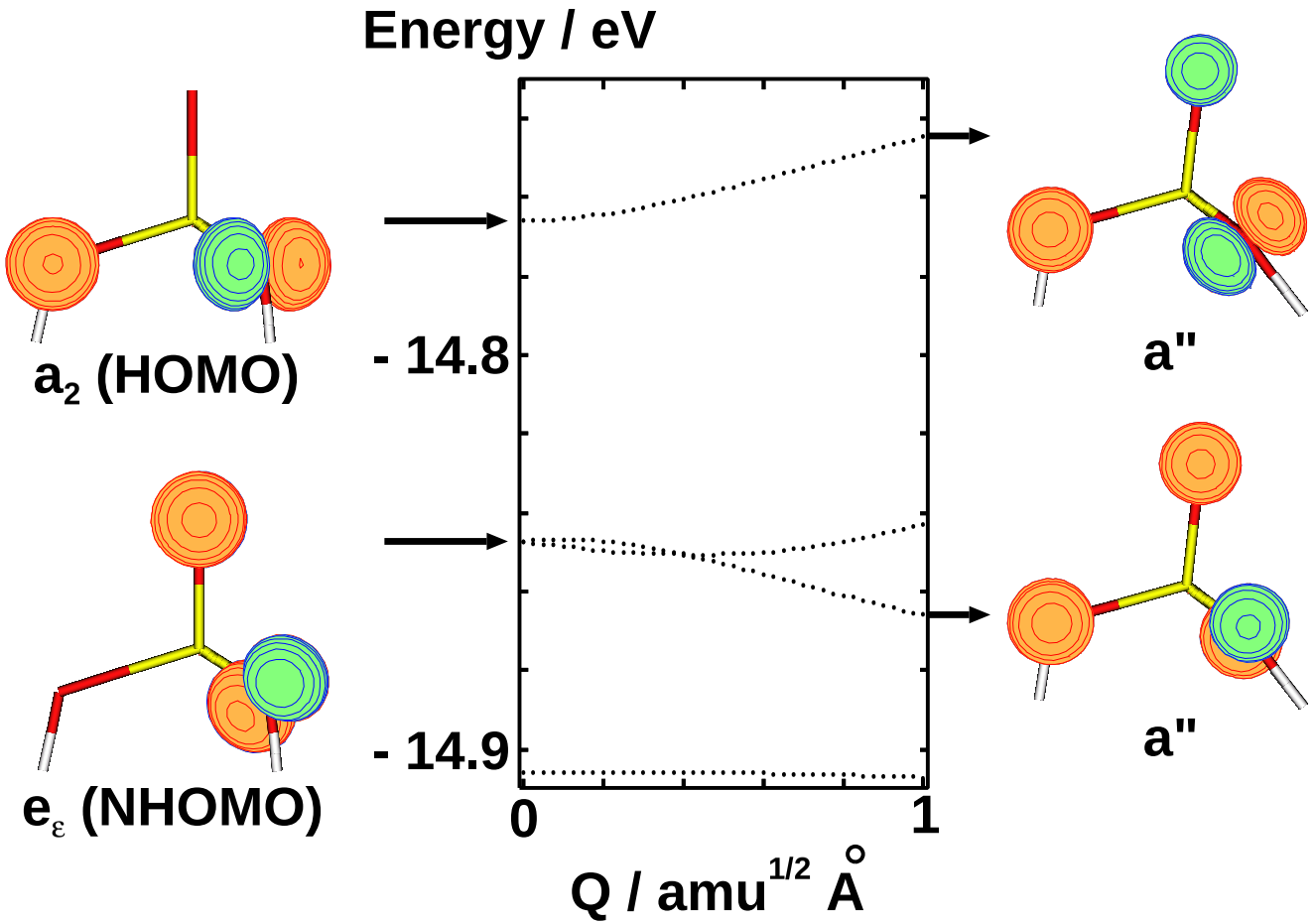

FIG. 4: Sato et. al

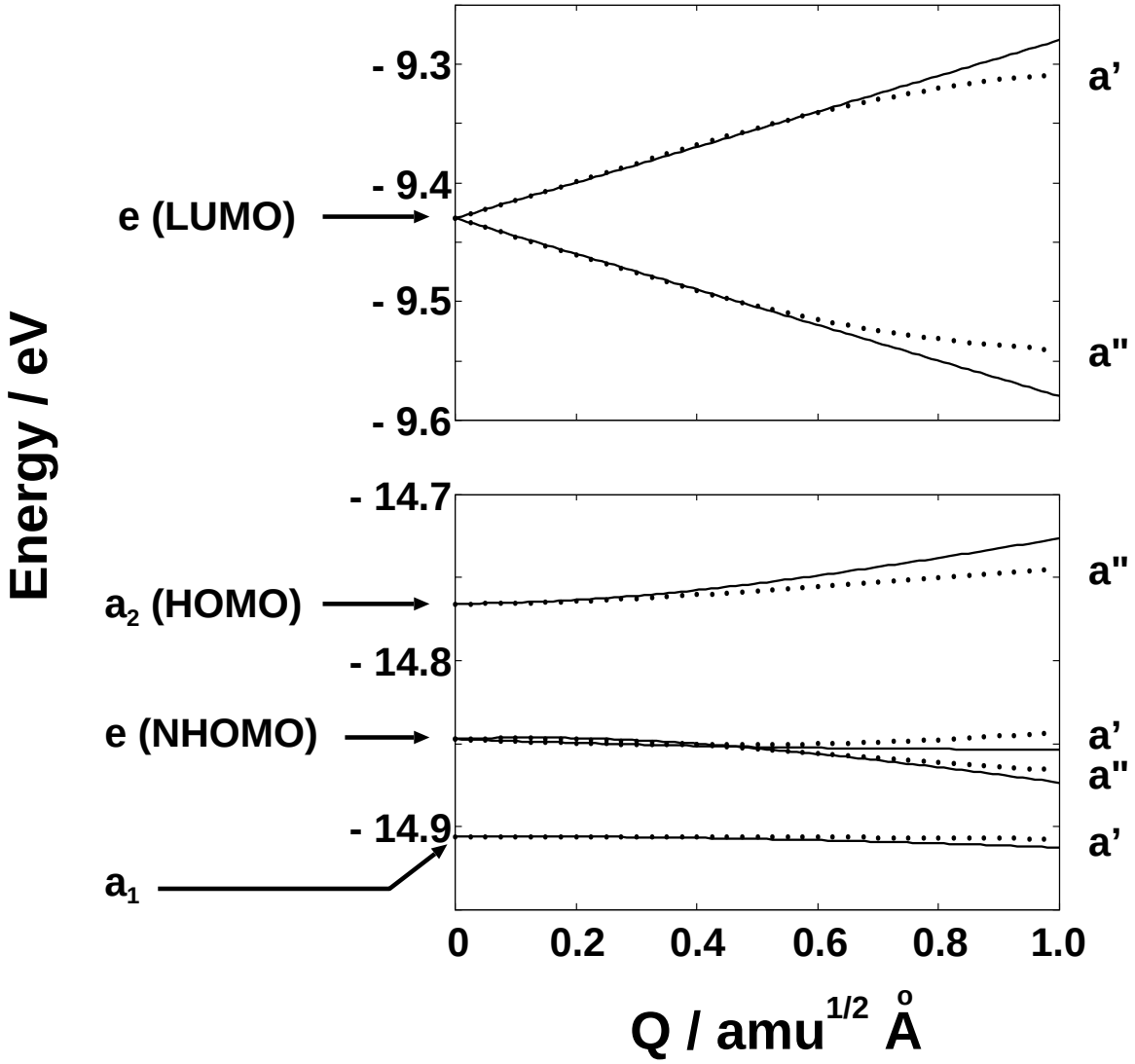

FIG. 5: Sato et. al

Figure captions

FIG. 1: (a) Isolated active species of highly dispersed vanadium oxide supported on silica, VO_4/SiO_2. There are two kinds of oxygen, terminal oxygen O_t and basal oxygen O_b. (b) Model molecule H_3VO_4.

FIG. 2: Vibrational a_1 and e modes of the X^1A_1 state.

FIG. 3: Schematic representation of the optimized structures and the Jahn-Teller potential surface in the triplet state. (a) The triangle indicates three basal oxygens (b) Cross section of the potential along the line between the minimum and the saddle point. At the center, the potential curves conically intersect.

FIG. 4: Orbital mixing of the HOMO a_2 and NHOMO e.

FIG. 5: Orbital energy calculated using the extended Hückel method (dotted lines) and calculated energy spectrum of the vibronic Hamiltonian with the parameters(solid lines) as a function of the $e(3)$ normal coordinate.